

## One-loop effects in supergravity models with an additional U(1)

D. A. Demir and N. K. Pak

*Department of Physics, Middle East Technical University, 06531, Ankara, Turkey*

(Received 9 December 1997; published 4 May 1998)

For an Abelian extended supergravity model, we investigate some important low-energy parameters:  $\tan \beta$ , the  $Z$ - $Z'$  mixing angle, lightest  $CP$ -even Higgs mass bound,  $Z'$  mass, and effective  $\mu$  parameter. By integrating the renormalization group equations from the string scale down to the weak scale we construct the scalar potential and analyze the quantities above at the tree- and one-loop levels by including the contributions of top squarks and top quark in the effective potential. [S0556-2821(98)02211-5]

PACS number(s): 04.65.+e, 12.60.Jv

### I. INTRODUCTION

There are several reasons for considering additional U(1) symmetries and their associated extra  $Z$  bosons. Such additional U(1)'s arise after the breaking of grand unified theories (GUT's) [for example  $E(6)$ -based rank-5 models], or in string compactifications. In addition to justifying the underlying model, more importantly, additional U(1)'s would also solve the minimal supersymmetric standard model (MSSM)  $\mu$  problem when broken around the weak scale. Indeed, as was already argued in [1], in a large class of string models, the breaking scale of the extra U(1)'s come out to be below 1 TeV.

The phenomenologically viable models should satisfy two conditions at the string scale: First, the extra U(1) should be nonanomalous and should not acquire a mass from the string or hidden sector dynamics; namely, its mass must come from the gauge symmetry breaking in the observable sector. Secondly, all scalar soft mass squareds must be positive and of similar magnitude. The latter holds in a gravity-mediated supersymmetry (SUSY) breaking scheme, where the mass scale is given by the gravitino mass, not necessarily so, however, in gauge-mediated SUSY breaking schemes.

Soft terms, parametrizing our ignorance of the origin of the SUSY breaking, can be obtained from a general supergravity (SUGRA) Lagrangian in the  $M_{Pl} \rightarrow \infty$  limit [2,3]. Although the minimal SUGRA predicts universal soft terms, in general SUGRA theories (see Ref. [4], and references therein) and superstring theories [5] it is possible to have nonuniversal soft terms. Thus, considering such explicit examples, one is free to consider nonuniversal boundary conditions [6], without referring to the particular case of universality.

For testing such extra U(1) models in machines of the near-future, the tree-level potential is clearly not sufficient; one has to take into account the radiative corrections to have a meaningful model at these energies. Among other methods [7], the effective potential approach proved to be an elegant and simple way of incorporating the radiative corrections to the scalar potential [8,9], which we will adopt in this work as well.

This work is organized as follows. In Sec. II we shall first describe the model at the SUGRA scale. Using one loop renormalization group equations (RGE's) we shall obtain all the low-energy potential parameters as functions of their

SUGRA scale values. After discussing the requirements on the low-energy potential for phenomenological viability, we determine the appropriate SUGRA scale parameter space. We do this with a minimal amount of nonuniversality. That is, we allow for nonuniversality only between Higgs doublets and remaining scalars; in particular, we choose doublet soft mass squareds to be equal and one order of magnitude smaller than the others.

In Sec. III we consider the issue of radiative corrections. Out of all fields which can contribute to the effective potential, we consider top quark and top squark contributions, and neglect the remaining fields. We assume that the log effects which are accounted for in solving the RGE's, are enough to take into account the effects of Higgs, neutralino, chargino, and vector boson loops, at least for calculating the low-lying mass spectrum [10].

In Sec. IV we work out the one-loop potential numerically, and graph the tree- and one-loop results together to enable a comparative discussion of the effects of the radiative corrections.

In Sec. V we discuss the results of the work in the light of accelerators of the near-future and MSSM and NMSSM predictions.

### II. LOW-ENERGY TREE-LEVEL POTENTIAL

As is well known, the fundamental SUGRA scale  $M = M_{Pl}/\sqrt{8\pi}$  is approximately one order of magnitude larger than the MSSM coupling constant unification level  $M_U \approx 10^{16}$  GeV [11]. However, the threshold effects [13,14] can close the gap, and thus, in the following we shall choose the MSSM unification scale  $M_U$  as the starting point of the analysis at which the initial conditions of the potential parameters are specified. We reconsider a general, anomaly free, Abelian extended SUSY model which was discussed in [12] already. The model is specified by an Abelian extension of the MSSM gauge group:  $G = SU(3)_c \times SU(2)_Y \times U(1)_{Y'} \times U(1)_{Y''}$  with the couplings  $g_3, g_2, g_Y, g_{Y'}$ , respectively. The particle content for one family is given by the left-handed chiral superfields:  $\hat{L} \sim (1, 2, -1/2, Q'_L)$ ,  $\hat{E}^c \sim (1, 1, 1, Q'_E)$ ,  $\hat{Q} \sim (3, 2, 1/6, Q'_Q)$ ,  $\hat{U}^c \sim (\bar{3}, 1, -2/3, Q'_U)$ ,  $\hat{D}^c \sim (\bar{3}, 1, 1/3, Q'_D)$ . The Higgs sector contains the SU(2) doublets  $\hat{H}_1 \sim (1, 2, -1/2, Q'_1)$  and  $\hat{H}_2 \sim (1, 2, 1/2, Q'_2)$ , and the SM singlet  $\hat{S} \sim (1, 1, 0, Q'_S)$ .

The superpotential for the model is given by

$$f = h_s^0 \hat{S} \hat{H}_1 \cdot \hat{H}_2 + h_t^0 \hat{U}^c \hat{Q} \cdot \hat{H}_2, \quad (1)$$

where the family mixings are ignored. We kept only the top and Higgs Yukawa couplings, as the Yukawa couplings of the other fermions are much smaller. The existence of  $U(1)_{Y'}$  group makes the model totally different from NMSSM by forbidding an elementary  $\mu$  term and an  $S^3$  term (so that the superpotential does not have a  $Z_3$  symmetry).

Without specializing to a particular class of string compactifications, we parametrize the supersymmetry breaking by considering the most general soft supersymmetry breaking terms

$$\begin{aligned} V_{\text{soft}} = & m_1^2 |H_1|^2 + m_2^2 |H_2|^2 + m_S^2 |S|^2 + m_U^2 |\tilde{t}_L^c|^2 \\ & + m_Q^2 |\tilde{Q}|^2 - h_s^0 A_s^0 (S H_1 \cdot H_2 + \text{H.c.}) \\ & - h_t^0 A_t^0 (\tilde{t}_L^c \tilde{Q} \cdot H_2 + \text{H.c.}) + \sum_a M_a^0 \lambda^a \lambda^a. \end{aligned} \quad (2)$$

Here  $\lambda^a$  are gauginos with the masses  $M_a^0$ , and  $\tilde{t}_L^c$  and  $\tilde{Q}$  are the scalar components of  $\hat{U}^c$  and  $\hat{Q}$ , respectively. The superscript on each quantity designates its value at the SUGRA scale which is determined by the vacuum expectation values (VEV's) of the hidden sector fields (moduli and dilaton fields, in the case of string compactifications), modulo the threshold corrections.

The scalar components of the Higgs superfields are assigned the following representation under  $SU(2)$  group:

$$\hat{H}_1 \rightarrow H_1 = \begin{pmatrix} H_1^0 \\ H_1^- \end{pmatrix}, \quad \hat{H}_2 \rightarrow H_2 = \begin{pmatrix} H_2^+ \\ H_2^0 \end{pmatrix}, \quad \hat{S} \rightarrow S. \quad (3)$$

Adding to  $V_{\text{soft}}$  the usual  $F$  and  $D$  terms of the associated group factors, one obtains the full scalar potential, whose Higgs part reads

$$\begin{aligned} V_0 = & m_1^2 |H_1|^2 + m_2^2 |H_2|^2 + m_S^2 |S|^2 + \lambda_{11}^0 |H_1|^4 + \lambda_{22}^0 |H_2|^4 \\ & + \lambda_S^0 |S|^4 + \lambda_{12}^0 |H_1|^2 |H_2|^2 + \lambda_{1S}^0 |H_1|^2 |S|^2 + \lambda_{2S}^0 |H_2|^2 |S|^2 \\ & - h_s^0 A_s^0 (S H_1 \cdot H_2 + \text{H.c.}) \end{aligned} \quad (4)$$

The terms involving parameters  $\lambda_i^0$  come from the supersymmetric part of the Lagrangian consisting of  $F$  and  $D$  terms, and their explicit expressions are:

$$\lambda_1^0 = \frac{1}{8} G_0^2 + \frac{1}{2} g_{Y'}^2 Q_1'^2, \quad (5)$$

$$\lambda_2^0 = \frac{1}{8} G_0^2 + \frac{1}{2} g_{Y'}^2 Q_2'^2,$$

$$\lambda_S^0 = \frac{1}{2} g_{Y'}^2 Q_2'^2,$$

$$\lambda_{12}^0 = -\frac{1}{4} G_0^2 + g_{Y'}^2 Q_1' Q_2' + h_s^0,$$

$$\lambda_{1S}^0 = g_{Y'}^2 Q_1' Q_2' + h_s^0,$$

$$\lambda_{2S}^0 = g_{Y'}^2 Q_2' Q_2' + h_s^0,$$

where  $G^0 = \sqrt{g_2^2 + g_{Y'}^2}$ . As there is no experimental constraint on  $U(1)_{Y'}$  group,  $g_{Y'}$  is arbitrary. However, for realistic models it is expected that  $g_{1'} \sim g_1$  [15], so we assume the unification of  $g_{1'}$  with the other gauge couplings at the the MSSM unification scale  $M_U$  [11]. Using the trace formulas for the fermion sector

$$\text{Tr}[Q_{\text{color}}^2] = \text{Tr}[Q_{\text{isospin}}^2] = 2, \text{Tr}[Y^2] = \frac{10}{3},$$

$$\text{Tr}[Y'^2] = 6Q_Q'^2 + 3(Q_U'^2 + Q_D'^2) + 2Q_L'^2 + Q_E'^2 \quad (6)$$

we normalize the gauge couplings such that, at  $M_U$ , they satisfy

$$g_3^0 = g_2^0 = g_1^0 = g_{1'}^0 = g^0, \quad (7)$$

with the normalized  $U(1)_Y$  and  $U(1)_{Y'}$  couplings

$$\begin{aligned} g_1^0 &= \sqrt{\frac{5}{3}} g_{Y'}^0, g_{1'}^0 \\ &= \sqrt{\frac{6Q_Q'^2 + 3(Q_U'^2 + Q_D'^2) + 2Q_L'^2 + Q_E'^2}{2}} g_{Y'}^0. \end{aligned} \quad (8)$$

In obtaining the renormalization group flow of the parameters of the potential we shall consider one-loop RGE's which were listed in Appendix A of Ref. [12]. We assume that the scale of SUSY breaking is around the weak scale, and thus we integrate RGE's of a softly broken SUSY model from the SUGRA scale down to the weak scale directly. Among the RGE's the most complicated ones are those involving Yukawa couplings  $h_s$  and  $h_t$  which obey coupled nonlinear equations. The top Yukawa coupling  $h_t$  reaches its fixed point value of  $h_t \sim 1 - 1.2$  almost independently of the initial conditions  $h_s^0$  and  $h_t^0$ . Corresponding to this  $h_s$  takes values around 0.6–0.8. On the other hand, the RGE's of soft masses, being linear, can be solved exactly as a function of their initial conditions, for given  $h_s^0$  and  $h_t^0$ . Finally, as a by-product of the coupling constant unification, it is natural to assume a common mass  $M_{1/2}$  for all gauginos at the SUGRA scale.

In constructing the solutions of RGE's one needs to specify the  $U(1)_{Y'}$  charges of the fields. Without referring to specific  $E(6)$  based charge assignments, one can relate different  $U(1)_{Y'}$  charges to each other by imposing the cancellation of the triangular anomalies together with the gauge invariance of the potential. The superpotential in Eq. (1) includes only the top and Higgs trilinear mass terms, and thus we shall require the gauge invariance for these vertices only, leaving the other would-be vertices (such as  $\hat{E}^c \hat{L} \cdot \hat{H}_1$ ) unconstrained. Then the solution of  $U(1)_{Y'}$  charges reads

$$\begin{aligned} Q'_S &= -(Q'_1 + Q'_2), & Q'_U &= (Q'_1 - 3Q'_2)/3, \\ Q'_D &= (Q'_1 + 3Q'_2)/3, \\ Q'_E &= -(Q'_1 - Q'_2), & Q'_Q &= -Q'_1/3, & Q'_L &= -Q'_2, \end{aligned} \quad (9)$$

which fix all but two ( $Q'_1$  and  $Q'_2$ ) of the  $U(1)_{Y'}$  charges. The advantageous side of this solution set is that it leaves the  $U(1)_{Y'}$  charges of Higgs doublets free, which will be important in analyzing the mixing angle of  $Z$  boson and  $U(1)_{Y'}$  gauge boson. We give this solution for the third family, and assume vanishing  $U(1)_{Y'}$  charges for the first two families. This is allowed in non-geometrical string compactifications (such as free-fermionic models), where a given Higgs doublet couples only one family [16]. As will be discussed later on, third family coupling of  $U(1)_{Y'}$  is important in analyzing the  $Z'$  models with CERN  $e^+e^-$  LEP constraints. Finally, for future use, we make the choice  $Q'_1 = Q'_2 = -1$  in Eq. (9) which fix all of the  $U(1)_{Y'}$  charges. Then, the solution of RGE's, with the initial values  $h_s^0 = h_t^0 = \sqrt{2}g^0$  for Yukawa couplings, read:

$$\begin{aligned} h_s &= 0.595, \\ h_t &= 1.028, \\ A_s &= 0.42A_s^0 - 0.272A_t^0 - 0.285M_{1/2}, \\ A_t &= -0.045A_s^0 + 0.128A_t^0 + 1.755M_{1/2}, \\ m_1^2 &= -0.064A_s^0{}^2 + 0.036A_s^0A_t^0 + 0.007A_t^0{}^2 - 0.01A_s^0M_{1/2} \\ &\quad + 0.019A_t^0M_{1/2} + 0.52M_{1/2}^2 + 0.047(m_Q^0{}^2 + m_U^0{}^2) \\ &\quad - 0.16m_s^0{}^2 + 0.84m_1^0{}^2 - 0.11m_2^0{}^2, \quad (10) \\ m_2^2 &= -0.038A_s^0{}^2 + 0.037A_s^0A_t^0 - 0.048A_t^0{}^2 + 0.045A_s^0M_{1/2} \\ &\quad - 0.19A_t^0M_{1/2} - 2.47M_{1/2}^2 - 0.41(m_Q^0{}^2 + m_U^0{}^2) - 0.1m_s^0{}^2 \\ &\quad - 0.1m_1^0{}^2 + 0.485m_2^0{}^2, \\ m_S^2 &= -0.128A_s^0{}^2 + 0.072A_s^0A_t^0 + 0.014A_t^0{}^2 - 0.021A_s^0M_{1/2} \\ &\quad + 0.039A_t^0M_{1/2} + 0.081M_{1/2}^2 + 0.094(m_Q^0{}^2 + m_U^0{}^2) \\ &\quad + 0.68m_s^0{}^2 - 0.32m_1^0{}^2 - 0.22m_2^0{}^2, \\ m_U^2 &= 0.017A_s^0{}^2 + 0.0005A_s^0A_t^0 - 0.037A_t^0{}^2 + 0.037A_s^0M_{1/2} \\ &\quad - 0.139A_t^0M_{1/2} + 3.27M_{1/2}^2 - 0.306m_Q^0{}^2 + 0.69m_U^0{}^2 \\ &\quad + 0.038m_s^0{}^2 + 0.038m_1^0{}^2 - 0.27m_2^0{}^2, \\ m_Q^2 &= 0.009A_s^0{}^2 + 0.0002A_s^0A_t^0 - 0.018A_t^0{}^2 + 0.019A_s^0M_{1/2} \\ &\quad - 0.07A_t^0M_{1/2} + 4.72M_{1/2}^2 + 0.85m_Q^0{}^2 - 0.15m_U^0{}^2 \\ &\quad + 0.02m_s^0{}^2 + 0.02m_1^0{}^2 - 0.13m_2^0{}^2. \end{aligned}$$

As a result of the normalization of the gauge couplings the low-energy parameters are not very sensitive to the assign-

ments of the  $U(1)_{Y'}$  charges. For example, if one chooses a model with  $E(6)$  charge assignments, the results are affected only by a few percent. Thus, from a practical point of view, one can regard the above-listed solutions as independent of  $U(1)_{Y'}$  charge assignments. On the contrary, dependence of the low-energy parameters, especially the trilinear couplings, on the variations of the initial conditions of Yukawa couplings is important. In what follows we shall confine ourselves to  $h_s^0 = h_t^0 = \sqrt{2}g^0$  [16], as was already used in obtaining Eq. (10). The low-energy potential with the parameters in Eq. (10) is a general one, and thus one has to specify the appropriate region of the parameter space to satisfy the phenomenological requirements existing at the weak scale.

After the breaking of gauge symmetry down to  $SU(3)_c \times U(1)_{em}$ , there will arise two neutral massive gauge bosons  $Z$  and  $Z'$  whose mass matrix reads

$$(\mathcal{M}^2)_{Z-Z'} = \begin{pmatrix} M_Z^2 & \Delta^2 \\ \Delta^2 & M_{Z'}^2 \end{pmatrix}, \quad (11)$$

where

$$M_Z^2 = \frac{1}{4}G^2(v_1^2 + v_2^2), \quad (12)$$

$$M_{Z'}^2 = g_{Y'}^2(v_1^2Q_1^2 + v_2^2Q_2^2 + v_s^2Q_S^2), \quad (13)$$

$$\Delta^2 = \frac{1}{2}g_{Y'}G(v_1^2Q_1 - v_2^2Q_2), \quad (14)$$

and, Higgs VEV's are defined as

$$\langle H_1^0 \rangle = v_1/\sqrt{2}; \quad \langle H_2^0 \rangle = v_2/\sqrt{2}; \quad \langle S^0 \rangle = v_s/\sqrt{2}. \quad (15)$$

There are three main conditions that the vacuum state must satisfy: The  $W$  boson mass must remain at its LEP1 value, as the model is extended only in the neutral direction; the color and charge symmetries must remain unbroken; the  $Z$ - $Z'$  mixing angle  $\alpha$  must be below a few  $\times 10^{-3}$  as otherwise the LEP1 value of  $M_Z$  is destructed.

The first condition can be satisfied using the fact that the potential (4) has a common mass scale defined by the gravitino mass, as the soft SUSY breaking terms in Eq. (2) are generated by the SUGRA breaking. Thus, the mass scale of the potential  $m_0$  (proportional to the gravitino mass), can be factored out and the remaining dimensionless potential can be minimized freely. The first condition above can then be met by imposing the constraint

$$m_0\sqrt{f_1^2 + f_2^2} = 246 \text{ GeV}, \quad (16)$$

where  $f_1$  and  $f_2$  are the dimensionless  $H_1$  and  $H_2$  VEV's, which are defined as  $v_1 = m_0f_1$ ,  $v_2 = m_0f_2$ , and for future use  $v_s = m_0f_s$ .

The charge breaking can arise from both Higgs and squark sectors. In the Higgs sector, with the help of  $SU(2)$  symmetry, a possible  $\langle H_2^+ \rangle$  can be rotated away, and the charge breaking can be parametrized in terms of  $v_- = \langle H_1^- \rangle$ . As can be calculated easily, the potential prefers the charge preserving minimum, if  $\tilde{A} > 0$ , where

$$\tilde{A} = 2 \sin^2 \beta m_{H^\pm}^2, \quad (17)$$

$\tan\beta = v_2/v_1$ , and  $m_{H^\pm}^2$  is the charged Higgs boson mass-squared. Consequently, in what follows we shall work in that portion of the parameter space where the charged Higgs boson has real mass, so that the charge breaking in the Higgs sector is avoided.

When, at least one of  $\langle \tilde{t}_L^c \rangle$ ,  $\langle \tilde{Q} \rangle$ , take a nonzero value, both color and charge symmetries are broken. To prevent the formation of such a minimum, one has to have a certain hierarchy between the top trilinear coupling  $A_t$  and the soft squark mass parameters. In fact, the usual criterium [17]  $h_t^2 A_t^2 < 3(m_{\tilde{Q}}^2 + m_{\tilde{U}}^2 + m_2^2)$  must hold at a scale  $Q \sim A_t/h_t$ . More importantly, when the squark masses go negative, a charge and/or color breaking minimum will be developed, even if it is secondary. When analyzing the low-energy potential, we shall always keep these conditions in mind.

That the  $Z$ - $Z'$  mixing angle is to be small is a severe constraint on the vacuum state. The  $Z$ - $Z'$  mixing angle  $\alpha$  is generated by the off-diagonal elements of the  $Z$ - $Z'$  mass matrix (10), and given by

$$\alpha = \frac{1}{2} \arctan \left( \frac{2\Delta^2}{M_{Z'}^2 - M_Z^2} \right). \quad (18)$$

There are mainly three regions of parameter space of the pure Higgs sector yielding a small  $\alpha$ .

(1) *Heavy  $Z'$  minimum.* As is seen from Eq. (18), when  $M_{Z'} \gg M_Z$ ,  $\alpha$  becomes small. This occurs in that portion of the parameter space satisfying

$$-m_S^2 \gg |m_1^2|, |m_2^2|, \quad (h_s A_s)^2 \quad (19)$$

for which Higgs VEV's behave as

$$v_s \sim \sqrt{-m_S^2/\lambda_s} \gg v_1, \quad v_2. \quad (20)$$

This ordering of the VEV's make  $\Delta^2$  small compared to  $M_{Z'}^2$ , whereby producing a small mixing angle. This mechanism does not require any relationship among the soft masses  $m_1^2$  and  $m_2^2$ , and charges  $Q'_1$  and  $Q'_2$ ; it utilizes only the ordering in Eq. (19).  $\tan\beta$ , however, is closely related to the values of charges  $Q'_1$ ,  $Q'_2$  and the values of the soft masses  $m_1^2$  and  $m_2^2$ . When  $-m_S^2$  takes higher and higher values, only  $U(1)_{Y'}$  gets broken, and other group factors remain unbroken. This introduces a mass scale  $Q = \sqrt{-m_S^2}$  between weak and SUGRA scales; remnants of the gauge group must be broken by a second stage around the weak scale. Before the occurrence of such an intermediate scale, large  $-m_S^2$  can create a relatively large  $\mu$  parameter, thus  $-m_S^2$  getting large values must be avoided.

(2) *Light  $Z'$  minimum.* As Eq. (18) suggests, another way of obtaining a small mixing angle would be to make  $\Delta^2$  small irrespective of the value of  $M_{Z'}$ . To obtain this kind of cancellation, one needs roughly  $v_1^2/v_2^2 \sim |Q'_2/Q'_1|$  which may be satisfied in some limited portion of the parameter space. However, unlike MSSM and similar to NMSSM, the existence of the trilinear coupling parameter  $h_s A_s$  opens a new avenue in obtaining an appropriate electroweak breaking. That is, when

$$h_s^2 A_s^2 \gg |m_1^2|, |m_2^2|, |m_S^2| \quad (21)$$

holds, all VEV's are drawn approximately to the same point:

$$v_1 \sim v_2 \sim v_s \sim A_s / (h_s \sqrt{2}). \quad (22)$$

If the  $U(1)_{Y'}$  charges of Higgs doublets satisfy  $Q'_2 = Q'_1$ , this large trilinear coupling-induced minimum cancels  $Z$ - $Z'$  mixing, allowing  $M_Z$  to be compatible with LEP1 data. Such a light  $Z'$  must show up in the  $Z$ -pole observables, and therefore parameters of the model can be constrained using LEP1 data. As a side remark, the passage of the trilinear coupling from lower values to higher ones (compared to the soft masses) is either a first order or second order phase transition, depending on the sign of  $m^2 = m_1^2 + m_2^2 + m_S^2$ . In fact, if  $m^2$  is positive, there is a first order phase transition occurring at the critical point  $A_s^{\text{crit}} = \sqrt{8m^2/3}$ .

(3) *Hybrid minimum.* One can obtain a phenomenologically viable minimum in all aspects by combining the parameter spaces of heavy  $Z'$  minimum and light  $Z'$  minimum. To do this, one can choose both  $-m_S^2$  and  $A_s^2$  large compared to other soft masses. As large  $A_s^2$  pushes all Higgs VEV's to the same point, and  $-m_S^2$  prefers a large SM-singlet VEV, when both  $-m_S^2$  and  $A_s^2$  are large, doublet VEV's [controlled by  $A_s$  via Eq. (22)] will approach to approximately the same value, and SM-singlet VEV [controlled by  $-m_S^2$  via Eq. (20)] will be much larger than them. Thus, this portion of the parameter space yields a small mixing angle together with a relatively heavy  $Z'$ . In the analyses below, we shall be mainly interested in this kind of parameter space and assume  $Q'_1 = Q'_2$ . Actually, when  $-m_S^2$  is large, one does not need this condition, as  $\Delta^2$  in Eq. (14) is already small compared to  $M_{Z'}^2$ . However, this kind of choice allows for the realization of the required minimum in a reasonable range of parameter values.

In the above mentioned low-energy analysis we have required a certain hierarchy among the potential parameters. However, as dictated by the solution of RGE's in Eq. (10), it is not realistic to consider such idealized cases since as one parameter changes, all others do too as a function of the initial conditions. Moreover, we need not only the Higgs sector parameters, but also the parameters of the squark sector as we shall calculate the one-loop squark contributions to the Higgs potential. Thus, one has to determine the SUGRA scale parameter space consistently by considering all the low-energy parameters simultaneously.

Once nonuniversality is permitted, one faces with a huge parameter space each point of which corresponds to some symmetry breaking scheme at low energies. The usual procedure for the determination of the appropriate portion of the parameter space, would be to trace the SUGRA-scale parameter space point-by-point, and pick up those yielding a viable minimum at low energies. However, with the low-energy parameters in Eq. (10), and the constraints implied by the hybrid minimum, we can determine the appropriate parameter space analytically. In accordance with the conditions coming from the hybrid minimum, we want to speed up  $-m_S^2$  and  $A_s$  compared to other mass parameters in terms of their dependence on a chosen SUGRA scale parameter. These two have three parameters  $A_s^0$ ,  $A_t^0$ , and  $M_{1/2}$  in common,

and we shall use  $A_s^0$  as a probe for determining the appropriate parameter space, by fixing other parameters with minimal amount of nonuniversality [6]. To slow down the  $A_s^0$  dependence of  $m_1^2$  and  $m_2^2$ , we make the following choice for  $m_1^{02}$  and  $m_2^{02}$ :

$$m_1^{02} \approx m_2^{02} \approx A_s^{02}/10. \quad (23)$$

For the remaining parameters we keep universality,

$$m_S^{02} = m_Q^{02} = m_U^{02} = A_t^{02}/3, \quad (24)$$

and finally we let  $M_{1/2} = A_t^0$ . Under these conditions, the low-energy parameters read

$$\begin{aligned} A_s &\approx 0.42A_s^0 - 0.58A_t^0, \\ A_t &\approx -0.045A_s^0 + 1.9A_t^0, \\ m_1^2 &\approx 0.026A_s^0A_t^0 + 0.53A_t^{02}, \\ m_2^2 &\approx 0.08A_s^0A_t^0 - 3.5A_t^{02}, \\ m_S^2 &\approx -0.18A_s^{02} + 0.05A_s^0A_t^0 + 0.43A_t^{02}, \\ m_Q^2 &\approx -0.0026A_s^{02} + 0.02A_s^0A_t^0 + 5.0A_t^{02}, \\ m_U^2 &\approx -0.0052A_s^{02} + 0.04A_s^0A_t^0 + 3.4A_t^{02}. \end{aligned} \quad (25)$$

As we see from these equations the quadratic  $A_s^{02}$  dependence of  $m_1^2$  and  $m_2^2$  are suppressed compared to those of the others with  $m_S^2$  being the fastest one among all concerning their  $A_s^{02}$  dependence. In the analysis below we shall vary

$$\zeta = A_s^0/A_t^0 \quad (26)$$

in a certain range of values, and determine  $A_t^0$  from the invariance of the  $W^\pm$  mass under such Abelian extensions of MSSM. When  $\zeta$  is small, except for  $m_2^2$ , all soft masses are positive, yielding a non zero and vanishing  $f_1, f_2$ . This is not an acceptable minimum, as the gauge symmetry is not broken completely. As  $\zeta$  increases,  $m_2^2$  starts overcoming the large negative threshold coming from [essentially the  $SU(3)_c$  gaugino masses, and  $H_1^0$  and  $S$  do develop nonzero VEV's. But still it may not yield a small enough mixing angle. Further increase of  $\zeta$  brings us to the sought minimum where  $0 \neq f_1 \sim f_2 \ll f_s$ . However, this increase cannot be maintained further as the squark masses turn to negative after overcoming their large positive mass thresholds dominated by the  $SU(3)_c$  gaugino. Negative squark masses cause charge and color breaking minima, even if secondary, so that this limiting case will be avoided below.

### III. ONE-LOOP CORRECTIONS

Until now our discussion has been based solely on the RGE-improved tree-level potential. However, quantum corrections beyond the log effects included in the RGE analysis are important. Especially the top-quark–top-squark sector gives the most important contribution due to the relatively

large value of the top-quark Yukawa coupling. To take such radiative corrections into account we shall follow effective potential approach [8,9] in which the radiatively corrected one-loop potential is given by

$$V_1 = V + \Delta V, \quad (27)$$

where the one-loop contribution has the Coleman-Weinberg form

$$\Delta V = \frac{1}{64\pi^2} \text{Str} \mathcal{M}^4 \ln \frac{\mathcal{M}^2}{Q^2}, \quad (28)$$

where Str is the usual supertrace and  $\mathcal{M}^2$  is the field dependent mass-squared matrix. We have transferred a renormalization scheme dependent constant into a redefinition of the renormalization scale  $Q^2$ . One notes that all the parameters in Eq. (27) are to be evaluated at the scale  $Q^2 \sim \mathcal{O}(v_1^2 + v_2^2)$ . Indeed, this is consistent with the RGE analysis of the last section as we have integrated them from the SUGRA scale down to the weak scale. In the loop expression Eq. (28) we consider only the contributions of top quarks and top squarks  $\tilde{t}_2, \tilde{t}_1$  whose masses are given by

$$\begin{aligned} m_t &= h_t |H_2^0|; \\ m_{\tilde{t}_{1,2}}^2 &= \frac{1}{2} \{ m_{11}^2 + m_{22}^2 \pm \sqrt{(m_{11} - m_{22})^2 + 4|m_{12}|^2} \}, \end{aligned} \quad (29)$$

where

$$\begin{aligned} m_{11} &= m_Q^2 + \lambda_{1t} |H_1|^2 + \lambda_{2t} |H_2|^2 + \lambda_{st} |S|^2 + \tilde{\lambda}_{1Q} |H_1^0|^2 \\ &\quad + \tilde{\lambda}_{2Q} |H_2^+|^2, \\ m_{22} &= m_U^2 + \lambda_{1u} |H_1|^2 + \lambda_{2u} |H_2|^2 + \lambda_{su} |S|^2, \\ m_{12} &= -h_t A_t H_2^{0*} + h_s h_t S^* H_1^{0*}, \end{aligned} \quad (30)$$

and the dimensionless coefficients

$$\begin{aligned} \lambda_{1t} &= -g_2^2/4 - g_Y^2/12 + g_Y^2 Q'_1 Q'_Q, \\ \lambda_{2t} &= -g_2^2/4 - g_Y^2/12 + g_Y^2 Q'_2 Q'_Q + h_t^2, \\ \lambda_{st} &= g_Y^2 Q'_S Q'_Q, \\ \lambda_{1u} &= g_Y^2 Q'_1 Q'_U, \\ \lambda_{2u} &= g_Y^2 Q'_2 Q'_U + h_t^2, \\ \lambda_{su} &= g_Y^2 Q'_S Q'_U, \\ \tilde{\lambda}_{1Q} &= g_2^2/2, \\ \tilde{\lambda}_{2Q} &= g_2^2/2 - h_t^2, \end{aligned} \quad (31)$$

follow from the colored sector of the full scalar potential. We shall calculate radiative corrections to the lightest  $CP$ -even Higgs mass bound, so we are interested in the

$CP$ -even scalar mass-squared matrix which can be obtained by evaluating  $\partial^2 V_1 / \partial \phi_i \partial \phi_j$  at the VEV's, in the basis  $(\text{Re}[H_1^0], \text{Re}[H_1^0], \text{Re}[S^0])$ .

Before going into a detailed numerical analysis, we first present a general discussion on the effects of the radiative corrections based on some approximate formulas. The top-quark–top-squark splitting  $S_{t\bar{t}} = \ln(m_{\bar{t}_1} m_{\bar{t}_2} / m_t^2)$  and top squark splitting  $S_{\bar{t}\bar{t}} = m_{\bar{t}_1}^2 - m_{\bar{t}_2}^2$  describe the most important contributions of the one-loop corrections. On the other hand, because of the choice of  $Q^2$ , the remaining  $\ln(m_t^2/Q^2)$  is not as important as the former ones. To extract some information about the effects of the loop corrections on the tree level parameters, one can expand the minimization equations in powers of top squark splitting and identify the renormalization effects on the tree-level quantities. In fact, to lowest order in stop splitting  $S_{\bar{t}\bar{t}}$ , and neglecting the terms involving the gauge couplings, one finds that the most important contributions come to  $A_s$ ,  $m_2^2$ , and  $\lambda_2$  which are given by

$$\begin{aligned}\hat{A}_s &= A_s + \beta_{h_t} S_{t\bar{t}} A_t, \\ \hat{m}_2^2 &= m_2^2 + \beta_{h_t} [(A^2 + A_t^2) S_{t\bar{t}} - A^2], \\ \hat{\lambda}_2 &= \lambda_2 + \beta_{h_t} S_{t\bar{t}} h_t^2,\end{aligned}\quad (32)$$

where  $\beta_{h_t} = [3/(4\pi)^2] h_t^2$ , and  $A^2 = m_Q^2 + m_U^2$ . Let us now discuss the implications of these one-loop corrections in the light of the RGE solution set in Eq. (25). As the first equation in Eq. (32) shows,  $A_s$  is strengthened by the loop corrections. However,  $A_s^0$  dependence of  $A_t$  is approximately one order of magnitude smaller than that of  $A_s$  so that one does not have a significant improvement for  $A_s$ , unless top-quark–top-squark splitting is large. The improvement in  $m_2^2$ ,  $\delta m_2^2 \sim \beta_{h_t} A^2 (S_{t\bar{t}} - 1)$  depends, in addition to  $A^2$  itself, on how large  $S_{t\bar{t}}$  is compared to unity. That is, if the top squark-masses are large compared to  $m_t$ , the top-quark–top-squark splitting can be large enough to give a significant contribution to  $m_2^2$ . Hence, both  $A_s$  and  $m_2^2$  get significantly improved if the top-quark–top-squark splitting is large enough. As one can read off from Eq. (25), for small  $\zeta$ , the squark soft masses are large due to the contribution of the  $SU(3)_c$  gaugino. Therefore,  $m_2^2$  is significantly improved by the loop corrections in this range of the  $\zeta$  values. However, we observe from Eq. (25) that for larger  $\zeta$  values  $A^2$  gets smaller and the loop contributions drop significantly. Finally, as dictated by Eq. (32),  $H_2$  quartic coupling  $\lambda_2$  is significantly improved by the radiative corrections if the top-quark–top-squark splitting is large enough. In the small  $\zeta$  limit, one has  $f_2 \sim \sqrt{-m_2^2/\lambda_2} \gg f_1, f_s$ , which clearly shows that tree-level  $f_2$  is larger than the loop-level one. This radiative reduction in  $f_2$  causes one-loop  $\tan \beta$  to drop:

$$\tan^2 \hat{\beta} = \tan^2 \beta \left( 1 - \tan \beta \frac{\beta_{h_t} [(A^2 + A_t^2 + 2m_t^2) S_{t\bar{t}} - A^2]}{A_s \mu_s} \right), \quad (33)$$

where the effective MSSM  $\mu$  parameter  $\mu_s = (h_s v_s) / \sqrt{2}$  is introduced. Indeed, with the contributions of  $\hat{m}_2^2$  and  $\hat{\lambda}_2$ , one-

loop  $\tan \beta$  is reduced compared to the tree-level one. However, the inverse  $\mu_s A_s$  dependence will force the loop contribution to drop rapidly after some  $\zeta$  values. In this sense, one expects tree- and loop-level  $\tan \beta$ 's be close to each other in the large  $\zeta$  regime.

At the tree-level, for small  $\zeta$ , one expects a relatively large mixing angle as the expected cancellation in  $\Delta^2$  does not occur. At the loop-level, however, because of the reduced  $\tan \beta$  one expects a smaller  $Z$ - $Z'$  mixing angle as can be seen from the form of  $\Delta^2$  in Eq. (14). Although in the large  $\zeta$  limit radiative correction to  $\tan \beta$  is diminished, due to the increase in  $v_s$  ( $-m_s^2$  increases) the loop-level  $Z$ - $Z'$  mixing angle will be still smaller than the tree-level one.

The lightest  $CP$ -even Higgs boson mass has the tree-level bound of

$$\begin{aligned}m_{h_1}^{2\max} &= M_Z^2 \cos^2 2\beta + (v_1^2 + v_2^2) \left[ \frac{h_s^2 \sin^2 2\beta}{2} \right. \\ &\quad \left. + g_{Y'}^2 (Q_1' \cos^2 \beta + Q_2' \sin^2 \beta) \right].\end{aligned}\quad (34)$$

Here the first term is the MSSM tree level bound, the  $h_s^2$  term is the NMSSM contribution ( $g_{Y'} = 0$  case), and finally the last term is the  $D$ -term contribution of the  $U(1)_{Y'}$  group. Using the same approximations that had lead us to Eq. (32), a straightforward calculation yields the following one-loop bound:

$$\hat{m}_{h_1}^{2\max} = m_{h_1}^{2\max} + \beta_{h_t} [(\mu_s \cos \beta + A_t \sin \beta)^2 + 4 S_{t\bar{t}} m_t^2]. \quad (35)$$

As we observe from this equation, the one-loop bound is always larger than the tree-level one. Since  $A_s^0$  dependence of  $A_t$  is weak, the main contribution to the bound comes from  $m_t$  and  $\mu_s$  terms, and it is maximized either by top-quark–top-squark splitting contribution, or by the  $\mu_s$  contribution. In fact, due to this  $\mu_s$  dependence it will be much larger in heavy  $Z'$  minimum than in light  $Z'$  minimum. In the parameter space we shall trace one expects the one-loop bound be dominated by  $m_t$  and  $\mu_s$  terms in the small and large  $\zeta$  regimes, respectively.

Had we included the entire particle spectrum and worked to all orders our results would be  $Q^2$  independent. The one-loop expressions for  $\hat{A}_s$  and  $\hat{m}_2^2$  in Eq. (32) are actually  $Q^2$  dependent and their dependence can be recovered by letting  $S_{t\bar{t}} \rightarrow S_{t\bar{t}} + \ln(m_t^2/Q^2)$ . Therefore, if for some choice of  $Q^2$ ,  $\ln(m_t^2/Q^2)$  happens to be important, one can analyze these two quantities by introducing the splitting function  $S_{Q\bar{t}} = \ln(m_{\bar{t}_1} m_{\bar{t}_2} / Q^2)$ . Similarly, in the expression for  $\tan \beta$ , except the for  $m_t^2$  term, one can make the replacement  $S_{t\bar{t}} \rightarrow S_{Q\bar{t}}$  to take into account its  $Q^2$  dependence. Unlike these,  $\hat{\lambda}_2$  in Eq. (32), and lightest Higgs boson mass bound in Eq. (35) are independent of  $Q^2$ , so they exhibit the same behavior for all  $Q^2$ . In general, all scalar mass-squared matrices are  $Q^2$  dependent, but the lightest  $CP$ -even Higgs boson mass bound turns out to be scale independent. In the RGE analysis assumed that the scale of the SUSY breaking  $M_{\text{SUSY}}$  is around the weak scale, so the choice of  $Q^2 \sim (v_1^2 + v_2^2)$  is

necessary for consistency of the analysis. Thus, we do not expect the  $Q^2$  dependence of the parameters to change the above mentioned predictions significantly.

Until now we have based our analysis on the approximate formulas which were obtained by assuming that the top-quark–top-squark splitting,  $\ln(m_{\tilde{t}}^2/Q^2)$ , and all gauge coupling dependent terms are negligibly small. These assumptions do not necessarily hold in the entire  $\zeta$  spectrum, and thus we need to have a detailed picture for the  $\zeta$  dependence of all these quantities.

#### IV. NUMERICAL ANALYSIS

In this section we shall investigate the effects of the radiative corrections on various quantities by an exact treatment of the problem using numerical techniques. To obtain the scalar mass matrices one has to calculate  $\partial^2 V_1 / \partial \phi_i \partial \phi_j$  evaluated at the VEV's. During the minimization we shall rescale all fields and parameters of mass dimension by  $A_t^0$ ; consequently the parameters of the potential depend on a single quantity,  $\zeta$  defined in Eq. (26). After minimizing the dimensionless potential, we recover the physical shell by requiring

$$A_t^0 = v / \sqrt{f_1^2 + f_2^2}, \quad (36)$$

where  $v = 246$  GeV is the Fermi scale. As we have already discussed in obtaining Eq. (16), this rescaling procedure works very well for the tree level potential [12] due to the uniqueness of the mass scale. However, radiative corrections do necessarily introduce an additional mass scale  $Q^2$ . Thus, the rescaling invariance of the tree-level potential does not hold at the loop level. Using Eq. (36), one would rescale the basic log in Eq. (28) as

$$\ln \frac{\mathcal{M}^2}{Q^2} = \ln \tilde{\mathcal{M}}^2 \frac{A_t^{02}}{Q^2}, \quad (37)$$

which clearly requires the knowledge of  $A_t^0$  which itself is something we aim to find. The determination of  $A_t^0$  thus requires a consistency analysis where one inserts a trial value in this rescaled log, and compares it with the resulting one after the minimization. This procedure goes on until trial and output values for  $A_t^0$  match. We have done this numerically, and the result is shown in Fig. 1 as a function of  $\zeta$ .

In the analysis below we shall present tree-level and one-loop quantities on the same graph for the sake of easy comparison. In each graph the free variable is  $\zeta$ , the ratio of the Higgs boson trilinear coupling to the top quark trilinear coupling at the SUGRA level. The starting value of  $\zeta$  is chosen to be that one for which none of the VEV's vanish. On the other hand, the maximum of  $\zeta$  is determined by its threshold value at which  $m_{\tilde{t}_2}^2$  turns to negative due to large  $v_s$  values.

This threshold shows up before squark soft masses turn to negative; so there is no danger of charge and/or color breaking in the range of  $\zeta$  values we shall consider below.

Figure 1 shows the  $\zeta$  dependence of  $A_t^0$  for tree- and loop-level analyses. While tree-level  $A_t^0$  peaks around  $\zeta = 7$  with a value 73 GeV, one-loop  $A_t^0$  peaks around  $\zeta = 8$  hitting the value of 82 GeV. As the VEV's leave the small  $\zeta$  regime

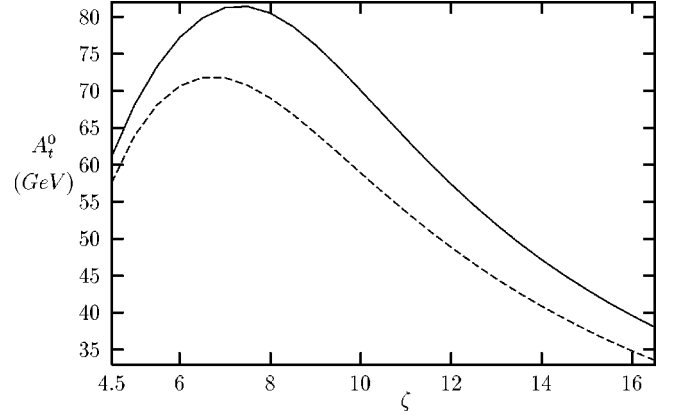


FIG. 1. Dependence of  $A_t^0$  on  $\zeta$  (solid line: one loop, dashed line: tree level).

(or  $f_2$  dominated regime), the sum  $f_1^2 + f_2^2$  approaches its minimum, as  $f_1$  and  $f_2$  are driven to close enough values by  $A_s$ . That  $A_t^0$  will be maximized around these  $\zeta$  values follows from Eq. (36). After passing by this maximization point, all of the mass parameters become proportional to the associated power of  $\zeta$ , as dictated by Eq. (25). Hence, in this ‘‘large  $\zeta$ ’’ regime, we expect dimensionless doublet VEV's be approximately proportional to  $\zeta$  because of which we observe an approximate  $1/\zeta$  falloff in Fig. 1. This kind of behavior in  $A_t^0$  reflects itself in all the relevant masses we shall discuss below. In solving the RGE's we have used the prescription  $M_{1/2} = A_t^0$ , which implies the weak scale masses of  $\sim 2.6 \times A_t^0$ ,  $0.8 \times A_t^0$ ,  $A_t^0/4$ , and  $A_t^0/10$  for  $SU(3)_c$ ,  $SU(2)$ ,  $U(1)_Y$ , and  $U(1)_{Y'}$  gauginos, respectively. Thus, depending on the present and future experimental limits on the gaugino masses of different group factors, one can restrict  $\zeta$  to a certain range of values, keeping in mind that the choice  $M_{1/2} = A_t^0$  itself is not necessarily unique.

We plot the  $\zeta$  dependence of  $\tan\beta$  in Fig. 2. As we observe from this figure, for small  $\zeta$  values, loop contributions really do push  $\tan\beta$  to smaller values. Again in agreement with our expectations, for large  $\zeta$ , both the tree level and loop results come closer rapidly, and gradually approach to unity. The difference between one-loop and tree-level  $\tan\beta$ 's fall below 1% after  $\zeta \sim 8$ .

In Fig. 3 we present the  $\zeta$  dependence of the  $Z$ - $Z'$  mixing

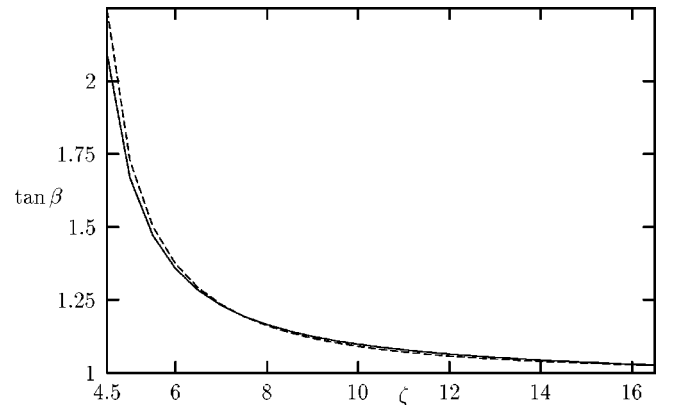


FIG. 2. Dependence of  $\tan\beta$  on  $\zeta$  (solid line: one loop, dashed line: tree level).

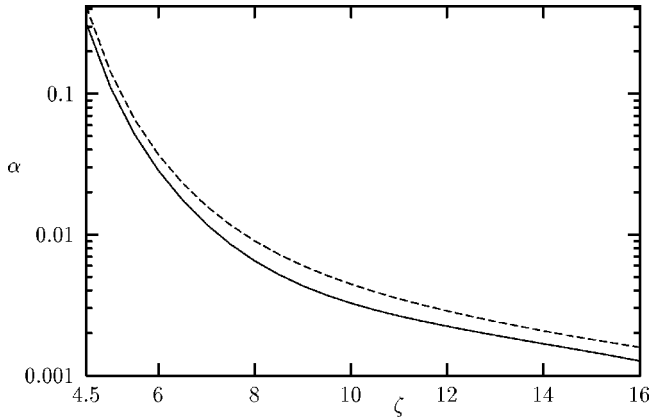


FIG. 3. Dependence of  $\alpha$  on  $\zeta$  (solid line: one loop, dashed line: tree level).

angle  $\alpha$ . In agreement with the predictions of the last section, the one-loop mixing angle is smaller than the tree level one everywhere. As we see from this figure, the phenomenological bound of  $\alpha_{\max} \sim \text{a few} \times 10^{-3}$  after  $\zeta \sim 7$  is comfortably satisfied after  $\zeta \sim 7$ . The last point about this figure is that for large  $\zeta$  values one-loop and tree-level results remain approximately parallel, indicating the fact that both doublet VEV's reach their limiting values controlled by  $A_s$ , and the SM-singlet VEV enter the  $-m_S^2$  dominated regime.

Another important quantity,  $M_{Z_2}$ , is shown in Fig. 4 as a function of  $\zeta$ . First, we see that loop corrections generally increase the  $Z_2$  mass in the entire  $\zeta$  range. Both tree-level and one-loop masses increase until  $\zeta \sim 10$  in accordance with  $A_t^0$  in Fig. 1. Likewise, parallel to the behavior of  $A_t^0$ ,  $M_{Z_2}$  decreases gradually after  $\zeta \sim 10$ , and is expected to saturate after some point due to the fact that the  $\zeta$  dependence of  $A_t^0$  and the dimensionless SM-singlet VEV are almost inversely proportional to each other in this range of  $\zeta$  values. The one-loop  $M_{Z_2}$  peaks at  $\zeta \sim 11$  by taking the value of  $\sim 405$  GeV; thus, it cannot increase indefinitely with  $\zeta$ . As expected, the tree-level  $M_{Z_2}$ , in similarity with the tree-level  $A_t^0$ , peaks at  $\zeta \sim 10$ , with a value  $\sim 330$  GeV. The values taken by  $M_{Z_2}$  depends crucially on the value of  $g_{Y'}$ . Under the normalization in Eq. (8), and the  $U(1)_{Y'}$  charge assignments in Eq. (9), the solution of the RGE's yield  $g_{Y'}/g_Y$

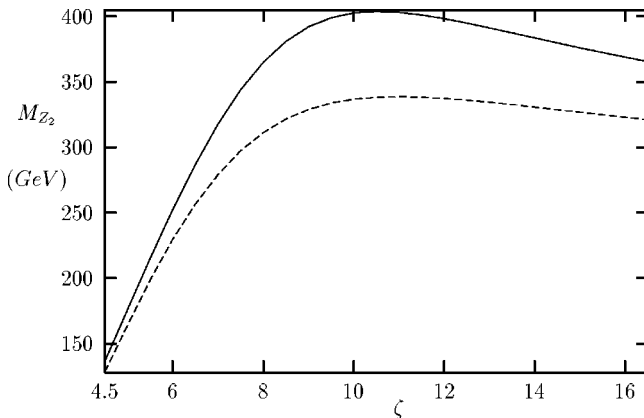


FIG. 4. Dependence of  $M_{Z_2}$  on  $\zeta$  (solid line: one loop, dashed line: tree level).

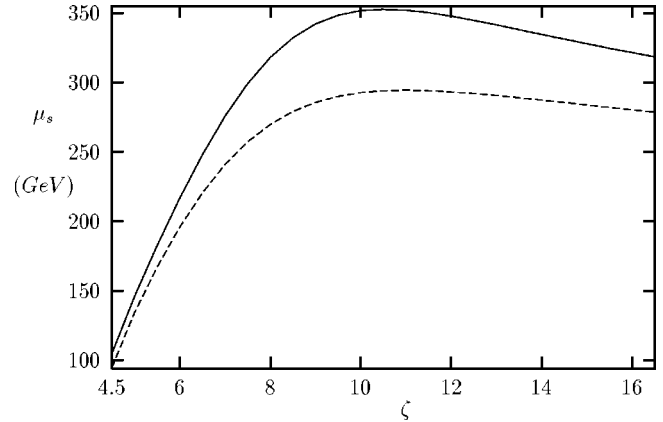


FIG. 5. Dependence of  $\mu_s$  on  $\zeta$  (solid line: one loop, dashed line: tree level).

$\approx 0.65$  at the weak scale. This ratio would push the value of  $M_{Z_2}$  above 600 GeV, if  $g_{Y'} = g_Y$  were the case. One notes that the recent Fermilab Tevatron result [18] giving  $M_{Z_2} \geq 590$  GeV would be well satisfied if  $g_{Y'}$  were equal to  $g_Y$ .

As explained in the Introduction, one of the basic aims of constructing such extended models is of course the dynamical formation of the MSSM  $\mu$  parameter. The effective  $\mu$  parameter in the present model has the  $\zeta$  dependence shown in Fig. 5, for which we have almost the same behavior observed in  $Z_2$  mass, as both are controlled by  $A_t^0$ . The one-loop  $\mu_s$  peaks around  $\zeta = 11$ , and takes the value  $\sim 350$  GeV at this point. Similarly, the tree level  $\mu_s$  peaks around  $\zeta = 10$  with a value  $\sim 280$  GeV.

Finally, in Fig. 6, we present the  $\zeta$  dependence of the lightest Higgs boson mass bound  $m_{h_1}^{\max}$  which is seen to satisfy the predictions of the last section. As we see from Eq. (34), the tree level bound depends solely on the doublet VEV's, so that after reaching the  $\tan \beta \sim 1$  regime the bound is maximized and saturated at  $m_{h_1}^{\max} \sim 118$  GeV. In the same way until leaving the small  $\zeta$  region, the one-loop bound also increases and hits the value  $\sim 125$  GeV in the far end of the total  $\zeta$  range. The fact that one-loop bound saturates much later than the tree-level one is due to the  $\mu_s$  dependence of the radiative corrections.

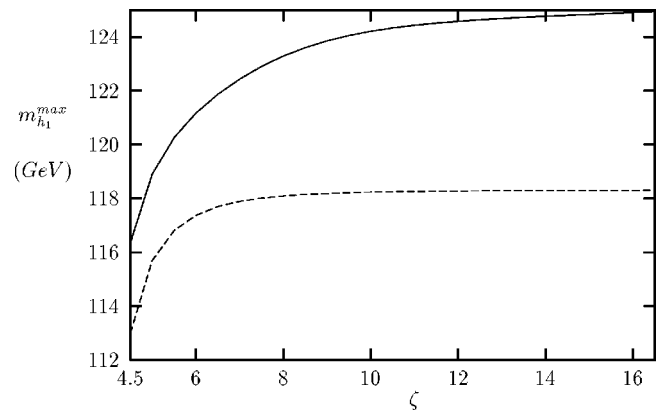


FIG. 6. Dependence of  $m_{h_1}^{\max}$  on  $\zeta$  (solid line: one loop, dashed line: tree level).

## V. CONCLUSIONS AND DISCUSSIONS

In this work we investigated one-loop contributions to certain low-energy quantities in the framework of the effective potential approach, using an RGE-improved radiatively corrected scalar potential, following from the superpotential in Eq. (1). However, derivation of the entire low-energy particle spectrum (such as top quark, bottom quark, and  $\tau$  masses) requires the study of a more general superpotential involving, in addition to the superpotential in Eq. (1), exotics predicted in most string models and nonrenormalizable quartic mass terms from which light fermion masses follow [16,19]. Here we have restricted ourselves mainly to the study of certain low-energy quantities determined by the Higgs sector of the model, for which the typical superpotential in Eq. (1) should suffice [12,19].

Among the low-energy quantities we have worked out, the  $Z'$  boson and lightest Higgs boson mass bound are of phenomenological importance. The search for  $Z'$  [20] will be one of the goals of the next generation of accelerators. In the near future, LEP II will be searching for the  $Z'$  boson in leptonic and  $WW$  channels. In addition to this, the CERN Large Hadron Collider (LHC) will search for  $Z'$  boson with quark-antiquark fusion processes. In general, the exclusion limits of  $Z'$  mass and its couplings depend on the model and collider parameters [21]. The  $U(1)_{Y'}$  charges of the present model are generation dependent, and thus, the constraints on its  $Z'$  boson is weaker than that of the generation independent ones. The  $Z$ - $Z'$  mixing angle (see Fig. 3) is small

enough to suppress the effects of  $Z'$  fermion couplings in the  $Z$ -pole observables [22]. The  $Z'$  mass in the present model has an upper bound of  $\sim 400$  GeV, and satisfies the presently existing phenomenological bounds.

The lightest Higgs mass bound turns out to be  $\sim 125$  GeV [23] in MSSM. In NMSSM, however, it is  $\sim 140$  GeV [10]. In the present model, it turns out to be  $\sim 125$  GeV. The bounds of the present model and MSSM practically coincide, however, the bound in the present model is expected to increase slightly if the next to next leading order (NNL) corrections are taken into account [23]. In the near future, the lightest Higgs boson will be discovered at LEP II if  $m_{h_1} \leq 95$  GeV, and at Fermilab in  $m_{h_1} \leq 120$  GeV after accumulating an integrated luminosity of  $25\text{--}30 \text{ fb}^{-1}$  [24].

In conclusion, we have analyzed the effects of the radiative corrections on the various low energy quantities in the present model by taking the contributions of top quarks and top squarks into account. As we have shown graphically, the one-loop improvement in the low energy parameters are in no way negligible. Moreover, the one-loop corrections support the satisfaction of the phenomenological requirements compared to the bare tree-level potential. The findings of the work will be tested in colliders of the near-future.

## ACKNOWLEDGMENTS

One of us (D.A.D.) thanks Paul Langacker for his helpful remarks at the earliest stages of this work.

- 
- [1] M. Cvetič and P. Langacker, Phys. Rev. D **54**, 3570 (1996).  
 [2] G. F. Giudice and A. Masiero, Phys. Lett. B **206**, 480 (1988).  
 [3] H. P. Nilles, Phys. Rep. **110**, 1 (1984).  
 [4] S. K. Soni and H. A. Weldon, Phys. Lett. **126B**, 215 (1983).  
 [5] A. Brignole, L. E. Ibanez, C. Munoz, and C. Scheich, Z. Phys. C **74**, 157 (1997); H. B. Kim and C. Munoz, Mod. Phys. Lett. A **12**, 315 (1997); A. Brignole, L. E. Ibanez, and C. Munoz, hep-ph/9707209.  
 [6] D. Matalliotakis and H. P. Nilles, Nucl. Phys. **B435**, 115 (1995).  
 [7] W. Hollik, hep-ph/9703231.  
 [8] M. Carena, M. Quiros, and C. E. M. Wagner, Nucl. Phys. **B461**, 407 (1996).  
 [9] M. Quiros, hep-ph/9703412.  
 [10] T. Elliot, S. F. King, and P. L. White, Phys. Lett. B **314**, 56 (1993); U. Ellwanger, *ibid.* **303**, 271 (1993).  
 [11] P. Langacker, hep-ph/9411247.  
 [12] M. Cvetič, D. A. Demir, J. R. Espinosa, L. Everett, and P. Langacker, Phys. Rev. D **56**, 2861 (1997).  
 [13] P. Langacker and N. Polonsky, Phys. Rev. D **52**, 3081 (1995).  
 [14] V. S. Kaplunovsky, Nucl. Phys. **B307**, 145 (1988).  
 [15] H. E. Haber and M. Sher, Phys. Rev. D **35**, 2206 (1987).  
 [16] A. E. Faraggi, Phys. Lett. B **274**, 47 (1992); **377**, 43 (1996).  
 [17] J. Ellis, J. F. Gunion, H. E. Haber, L. Roszkowski, and F. Zwirner, Phys. Rev. D **39**, 844 (1989).  
 [18] CDF Collaboration, F. Abe *et al.*, Phys. Rev. Lett. **79**, 2192 (1997).  
 [19] J. R. Espinosa, hep-ph/9707541.  
 [20] J. Hewett and T. Rizzo, Phys. Rep. **183**, 193 (1989).  
 [21] S. Riemann, hep-ph/9710564; A. Leike, hep-ph/9708436; T. G. Rizzo, hep-ph/9710229.  
 [22] K. S. Babu, C. Kolda, and J. March-Russel, hep-ph/9710441.  
 [23] J. A. Casas, J. R. Espinosa, M. Quiros, and A. Riotto, Nucl. Phys. **B167**, 3 (1995).  
 [24] A. Stange, W. Marciano, and S. Willenbrock, Phys. Rev. D **49**, 1354 (1994).